Macromolecules

NOTE

pubs.acs.org/Macromolecules

Functionalized Polylactide Film Surfaces via Surface-Initiated ATRP

F. J. Xu,* X. C. Yang, C. Y. Li, and W. T. Yang

State Key Laboratory of Chemical Resource Engineering, Key Laboratory of Carbon Fiber and Functional Polymers, Ministry of Education, College of Materials Science & Engineering, Beijing University of Chemical Technology, Beijing 100029, China

Supporting Information

1. INTRODUCTION

The application of synthetic polymers as biomaterials depends upon their interfacial properties and resultant interactions with cells and biological fluids *in vivo*. The ability to manipulate and control the surface properties of a biomaterial is of crucial importance in the design of biomedical materials.[1−5] Polylactide (PLA), a biodegradable and bioabsorbable polyester, has been widely adopted for scaffold fabrication in biomedical fields because of its excellent tissue biocompatibility.[6−9] However, the PLA-based scaffold surfaces lack the ability to interact with cells in a desired fashion. To improve cell adhesion and growth, some surface modification techniques, including UV irradiation,[6,7] electrostatic self-assembly,[8] alkaline treatment,[10,11] surface entrapment,[12] and plasma treatment,[6,13] have been employed for immobilizing some naturally extracellular matrix molecules (e.g., collagen, chitosan, and gelatin) onto PLA surfaces to induce specific cell interaction.

Covalent tethering of well-defined polymer brushes on a solid substrate is an effective method for modifying the surface properties.[14−17] Atom transfer radical polymerization (ATRP) is a recently developed "controlled" radical polymerization method.[18−20] Surface-initiated ATRP allows the preparation of well-defined dense polymer brushes and hence provides the high capacity of binding sites of functional molecules.[14,15,21] Recently, we explored surface-initiated ATRP of glycidyl methacrylate (GMA) to tailor the functionality of polycaprolactone (PCL) film surfaces.[21] The resultant plentiful epoxy groups of the well-defined PGMA brushes were used for coupling cell-adhesive collagen and RGDS to improve the cell-adhesion properties of the PCL film surface. In addition to the epoxy groups, it is also quite often to use the carboxyl groups for coupling biomolecules via esterification reactions. In comparison with self-assembled monolayer (SAM) with carboxyl termination, carboxyl polymer brushes have significantly higher biomolecule-binding capacities due to high concentrations of −COOH groups at the brush interfaces. Direct ATRP of (meth)acrylic acid may be hampered by the reaction of the monomer with the metal complex to form catalytically ineffective metal carboxylates.[18] Poly((meth)acrylic acid)) (P(AA) or P(MAA) brushes can be prepared alternatively via surface-initiated ATRP of *tert*-butyl-(meth)acrylate (followed by hydrolysis or pyrolysis of the *tert*-butyl ester protective groups) or of sodium (meth) acrylate instead of (meth)acrylic acid.[13,22] It was reported that the direct synthesis of P(AA) or P(MAA) brushes can be achieved via ATRP of sodium (meth)acrylate (MAAS), where the Na^+ ions can be quite easily removed by simply washing with water.[19,20,24]

Polyester is susceptible to slow chemical hydrolysis, and the resultant hydroxyl groups could be explored for the immobilization of ATRP initiators via esterification reaction on PCL surfaces.[21] Such an immobilization method could be used to tailor the functionality of PCL surfaces via surface-initiated ATRP of GMA.[21] However, such hydrolysis process of polyester also produced the corresponding −COOH groups, which may hamper the efficiency of the esterification reaction. In this work, a simple alternative two-step method was developed for the covalent immobilization of ATRP initiators on the PLA surfaces (Figure 1). It was well-known that the aminolysis process of polyester film surfaces (including PCL and PLA) with 1,6-hexanediamine can introduce the free amino and hydroxyl groups.[1,25] Both reactive groups are ready to react with 2-bromoisobutyryl bromide to produce the ATRP initiator-coupled PLA surfaces (the PLA-Br surfaces). Well-defined P(MAA) brushes (the PLA-*g*-P(MAA) surfaces) were subsequently prepared via surface-initiated ATRP of MAAS from the PLA-Br surfaces. The pendant carboxyl groups of P(MAA) chains were subsequently coupled with gelatin (one naturally extracellular matrix molecule) for improving the cell-adhesion properties of the PLA surfaces. Although the free amino from the aminolysis process of PLA can be used for the immobilization of gelatin, it was found that the dense pendant carboxyl groups of P(MAA) chains could provide much more binding sites of functional molecules to induce better cell-adhesion properties on the surface. The chemical compositions and cell-adhesion characteristics of the modified PLA film surfaces were characterized by X-ray photoelectron spectroscopy (XPS) and confocal laser scanning microscope (CLSM), respectively.

2. EXPERIMENTAL SECTION

2.1. Materials. Poly(DL-lactide) (PLA, M_w = 75 000−120 000), 1,6-hexanediamine, gelatin powder from porcine skin, 2-bromoisobutyryl bromide (98%), sodium methacrylate (methacrylic acid sodium salt, MAAS, 99%), copper(I) bromide (CuBr, 99%), copper(II) bromide ($CuBr_2$, >98%), *N*,*N*,*N*,*N*,*N*-pentamethyldiethylenetriamine (PMDETA, 99%), *N*-hydroxysuccinimide (NHS, 98%), and 1-ethyl-3-(3-(dimethylamino)propyl)carbodiimide hydrochloride (EDAC, 99%) were obtained from Aldrich Chemical Co. (Milwaukee, WI).

Received: January 23, 2011
Revised: February 28, 2011
Published: March 11, 2011

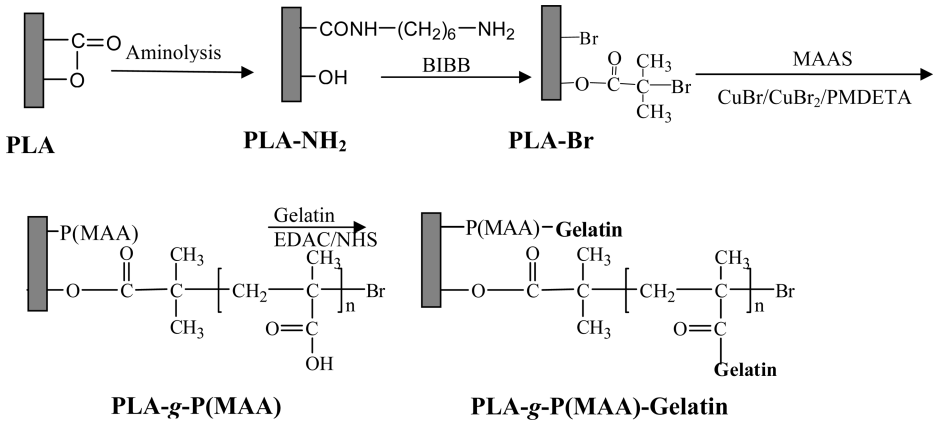

Figure 1. Schematic diagram illustrating the reaction of free amine and hydroxyl groups on the aminolyzed PLA film surface with 2-bromoisobutyrate bromide (BIBB) to produce the PLA-Br surface, surface-initiated ATRP of MAAS from the PLA-Br surface to produce the PLA-*g*-P(MAA) surface, and gelatin immobilization on the PLA-*g*-P(MAA) surface to produce the PLA-*g*-P(MAA)-gelatin surface.

2.2. Preparation of PLA Films. The PLA film was prepared by dissolving 2 g of PLA in 20 mL of dichloromethane. The polymer solution was then cast onto a glass substrate, and the solvent was removed by controlled evaporation at room temperature over a period of 24 h. The so-obtained pristine PLA film with a thickness of 50−100 μm was washed with copious amounts of a methanol/water (1/2, v/v) mixture. The dried PLA films were cut into specimen size of 2 cm × 2 cm for the subsequent surface reactions. The PLA films were subsequently immersed in 1,6-hexanediamine/2-propanol solution of 60 mg/mL for a predetermined period at 40 °C.[1,25] The aminolysis process produced the PLA-NH_2 films.

2.3. Surface-Initiated ATRP of MAAS. As shown schematically in Figure 1, the immobilization of ATRP initiator on the PLA-NH_2 film surface was accomplished via the reaction of the amino and hydroxyl groups with 2-bromoisobutyrate bromide (BIBB). The PLA-NH_2 films were introduced into 10 mL of dried hexane, followed by addition of 0.5 mL of 2-bromoisobutyryl bromide and 0.2 mL of dry pyridine. The reaction mixture was kept for 2 h at 0 °C and then at room temperature for 10 h to produce the 2-bromoisobutyryl-immobilized PLA surface (the PLA-Br surface). The PLA-Br substrate was washed repeatedly with a methanol/water (1/2, v/v) mixture and dried by pumping under reduced pressure. For the preparation of P(MAA) brushes on the PLA-Br surface, 3 g of MAAS and 6 mL of doubly distilled water were added to a Pyrex tube. The PMDETA, CuBr, and $CuBr_2$ were added in the [MAAS]:[CuBr]:[$CuBr_2$]:[PMDETA] molar feed ratio of 100:1:0.2:1.2. The mixture was stirred and degassed with argon for 20 min. The PLA-Br substrate was then introduced into the reaction mixture. The reaction was allowed to proceed at room temperature for 0.5−2 h to produce the PLA-*g*-P(MAA) surface. After the reaction, the PLA-*g*-P(MAA) surface was washed thoroughly with doubly distilled water to ensure the complete removal of the physically adsorbed reactants, prior to being dried under reduced pressure. Details on the surface-initiated ATRP had been described earlier.[14,24]

2.4. Immobilization of Gelatin. Gelatin, one naturally extracellular matrix molecule, is widely used in tissue engineering.[10,26,27] In this work, gelatin was immobilized onto the PLA-*g*-P(MAA) surface via carbodiimide chemistry to improve the cell-adhesion properties of the PLA film surface. The −COOH groups of the PLA-*g*-P(MAA) surface were preactivated for 2 h at room temperature in phosphate buffered saline (PBS, pH 7.4) solution, containing 1.0 mg/mL of NHS and 10 mg/mL of EDAC. The active substrates were then transferred to PBS solution containing 5 mg/mL of gelatin at 40 °C. The reaction was allowed to proceed for 12 h at 40 °C to produce the PLA-*g*-P(MAA)-gelatin surface. After the immobilization reaction, the films were washed sequentially with excess PBS and doubly distilled water at 40 °C to desorb the reversibly bound gelatin. These functionalized PLA surfaces were finally washed with sterilized PBS for further biological experiments.

2.5. Surface Characterization. The chemical compositions of the modified PLA film surfaces were characterized by X-ray photoelectron spectroscopy (XPS). The XPS measurements were performed on a Kratos AXIS HSi spectrometer using a monochromatized Al Kα X-ray source (1486.6 eV photons) and procedures similar to those described earlier.[14] The static water contact angles of the pristine and functionalized PCL film surfaces were measured at 25 °C and 60% relative humidity, using the sessile drop method with 3 μL water droplets, in a telescopic goniometer (Rame-Hart model 100-00-(230), Rame-Hart, Inc., Mountain Lakes, NJ).

2.6. Cell Culture. The cell-adhesion characteristics of the functionalized PLA surfaces were assessed by cell culture. The pristine and surface-modified PLA films were placed into the wells of a six-well culture plate. 3T3 fibroblasts (ATCC, Passage 27) were seeded into the wells at a density of 3 × 10^5 cells/well and incubated (in 4 mL of Dulbecco's modified eagle medium (DMEM) supplemented with 10% fetal bovine serum, 1 mM L-glutamine, and 100 U/mL penicillin (diluted from the 20 000 U/mL stock solution)) at 37 °C for 12−48 h under a humidified 5% CO_2 atmosphere. The surfaces after incubation were washed twice with PBS solution to remove the dead and loosely attached cells. 4′,6′-Diamidino-2-phenylindole (DAPI, Sigma) was used to stain the cell's nuclei for cell imaging.[28] The cultured cells on the film surfaces were stained for 10 min with 150 ng/mL DAPI in PBS before being further washed with methanol and PBS. DAPI-stained cells were observed by a confocal laser scanning microscope (CLSM) (Fluoview FV500, Olympus, Japan) using a 405 nm laser and a BP 430-490 emission filter. For cell number on each type of surface, the surfaces prewashed with PBS solution were incubated with trypsin−EDTA solution (0.25% trypsin, 1 mM EDTA) for 10 min at 37 °C to detach the cells. The detached cells were collected and counted using a hemocytometer.

3. RESULTS AND DISCUSSION

3.1. Immobilization of the ATRP Initiators. For the preparation of polymer brushes, the monolayer of initiators immobilized on the PLA film surface is indispensable. In this work, an aminolysis-based method was developed for the covalent immobilization of ATRP initiators on the polyester film surfaces. It is possible to introduce free amino groups on polyester film

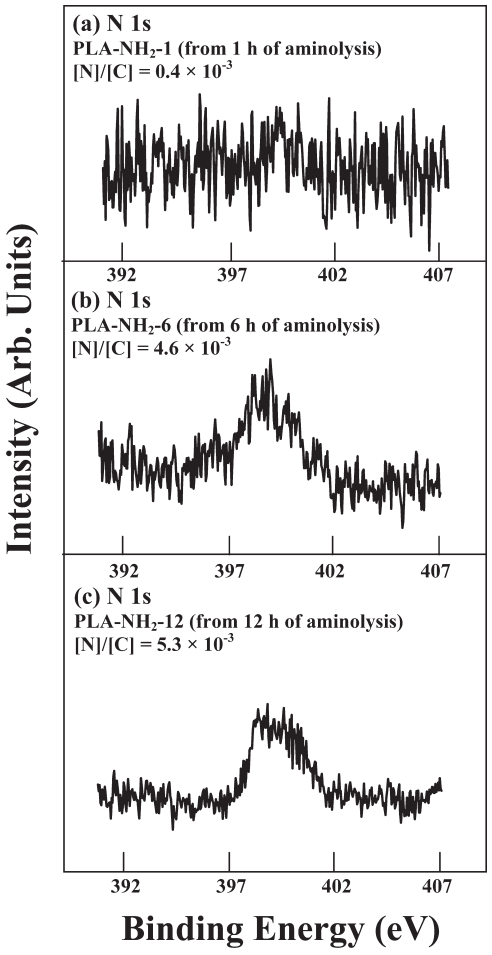

Figure 2. N 1s core-level spectra of the (a) PLA-NH_2-1 (from 1 h of aminolysis), (b) PLA-NH_2-6 (from 6 h of aminolysis), and (c) PLA-NH_2-12 (from 12 h of aminolysis) surfaces.

surfaces through the aminolysis reaction with diamine species.[1,25] One amine group can react the with −COO− species to produce the covalent bond, −CONH−, and the other $-NH_2$ group remains free. In addition, this aminolysis process also produces the hydroxyl-terminated chains. Both the resultant $-NH_2$ and −OH groups are ready to react with 2-bromoisobutyryl bromide (BIBB) to produce the ATRP initiator species (Figure 1). The pristine PLA film was immersed in 1,6-hexanediamine/2-propanol solution to induce surface aminolysis processes, producing the aminolyzed PLA-NH_2 film (Figure 1). In this work, the PLA-NH_2 film surfaces from 1, 6, and 12 h of aminolysis were denoted as the PLA-NH_2-1, PLA-NH_2-6, and PLA-NH_2-12 surfaces, respectively. The resultant amino and hydroxyl groups on the PLA-NH_2 film surfaces were used to react with BIBB to produce the corresponding ATRP initiator-coupled surfaces (the PLA-Br-1, PLA-Br-6, and PLA-Br-12 surfaces).

The chemical compositions of the PLA film surfaces at various stages of surface modification were determined by X-ray photoelectron spectroscopy (XPS). Figure 2 shows the N 1s core-level spectra of the (a) PLA-NH_2-1, (b) PLA-NH_2-6, and (c) PLA-NH_2-12 surfaces. With the increase in aminolysis time, the intensities of the N 1s signals increased substantially as expected. The surface [N]/[C] ratio (determined from the sensitivity factor-corrected N 1s and C 1s core-level spectral area ratio) increased from 0.4×10^{-3} for the PLA-Br-1 surface (from 1 h of aminolysis) to 5.3×10^{-3} for the PLA-Br-12 surface (from 12 h of aminolysis). These results confirmed that longer aminolysis can produce more surface amino and hydroxyl groups on the PLA-NH_2 surface. However, the N 1s signals (Figure 2b,c) of the PLA-Br-6 and PLA-Br-12 surfaces indicated that further prolonging the aminolysis time after 6 h at the present conditions did not lead obvious enhancement in the intensities of the resultant N 1s signals.

Figure 3 shows the C 1s core-level spectra of the (a) pristine PLA, (b) PLA-Br-1, (c) PLA-Br-6, and (d) PLA-Br-12 surfaces and the Br 3d core-level spectra of the (b′) PLA-Br-1, (c′) PLA-Br-6, and (d′) PLA-Br-12 surfaces. The C 1s core-level spectra can be curve-fitted into three peak components with binding energies (BE's) at about 284.6, 286.4, and 288.7 eV, attributable to the *C*−H, *C*−O (and *C*−Br), and *O* = C-O species, respectively.[29] A Br 3d signal at BE of about 69 eV, characteristic of covalently bonded bromine,[29] has appeared in the PLA-Br-1, PLA-Br-6 and PLA-Br-12 surfaces. With the increase in aminolysis time, the intensities of the Br 3d signals and C-O/C-Br peaks increased substantially as expected. The surface [Br]/[C] ratio (determined from the sensitivity factor-corrected Br 3d and C 1s core-level spectral area ratio) increased from 1.1×10^{-3} for the PLA-Br-1 surface to 8.1×10^{-3} for the PLA-Br-12 surface. Especially for the PLA-Br-6 and PLA-Br-12 surfaces, the weak O═*C*−N peak component with BE at about 287.4 eV, associated with the linkages between the PLA film surface and ATRP initiators, can be observed. The above results are consistent with those of Figure 2.

In order to estimate the ATRP initiator (alkyl bromide) density of the initiator-coupled PLA surfaces, the initiator density was first set an unknown value, ρ^* (Brs/nm^2). On the basis of the initiator density (ρ^*), mass density (ρ_1) of the 2-bromoisobutyrate (BIB) layer (1.0 g/cm^3), and molecular weight (M_1) of BIB (165.5 g/mol), the thickness (h) of the initiator layer was estimated to be about $0.27\rho^*$ ($h = \rho^* M_1/\rho_1$). From the mass density (ρ_2) of the PLA film (1.0 g/cm^3), the molecular weight (M_2) of the lactide (LA) repeat unit (144 g/mol), the stoichiometry ($C_6H_8O_4$) of the LA repeat unit, and the sampling depth (about 7.5 nm in an organic matrix[30]) of the XPS technique, the number (n) of the total C atoms per unit volume of the XPS probing depth ($V = 7.5$ nm^3) is about ($188.1 - 2.8\rho^*$) ($n = 4\rho^* + 6((7.5 - h)\rho_2/M_2)$).[31] On the basis of the [Br]/[C] ratios (r) of 1.1×10^{-3} (for the PLA-Br-1 surface, Figure 3b′), 6.7×10^{-3} (for the PLA-Br-6 surface, Figure 3c′), and 8.1×10^{-3} (for the PLA-Br-12 surface, Figure 3d′), the initiator densities (ρ^*) for the PLA-Br-1, PLA-Br-6, and PLA-Br-12 surfaces are finally estimated to be about 0.21, 1.26, and 1.52 initiators/nm^2 ($r = \rho^*/n$), respectively.

3.2. Surface-Initiated ATRP of MAAS. The physicochemical properties of PLA surfaces can be tuned by the choice of functional vinyl monomers. Recently, it was reported that poly((meth)acrylic acid) brushes can be readily prepared via aqueous surface-initiated ATRP of sodium (meth)acrylate.[19,20,24] In this work, methacrylic acid sodium salt (MAAS) polymer was immobilized on PLA substrates via surface-initiated ATRP as shown schematically in Figure 1. For surface-initiated ATRP, an excess amount of deactivating Cu(II) complex ($CuBr_2$) was added. This approach allows thicker polymer brushes to be grown at a faster rate in the presence of a higher monomer concentration because of the absence of accompanying homopolymerization in solution.[22,32] The molar feed ratio of

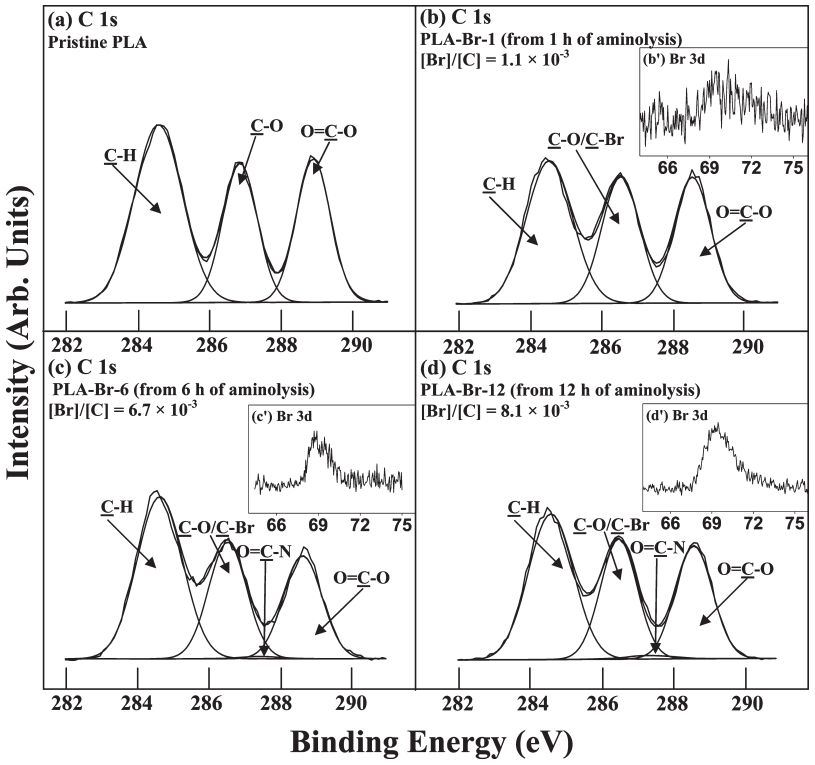

Figure 3. C 1s core-level spectra of the (a) pristine PLA, (b) PLA-Br-1 (from 1 h of aminolysis), (c) PLA-Br-6 (from 6 h of aminolysis), and (d) PLA-Br-12 (from 12 h of aminolysis) surfaces and Br 3d core-level spectra of the (b′) PLA-Br-1, (c′) PLA-Br-6, and (d′) PLA-Br-12 surfaces.

Table 1. Reaction Time, Grafting Yield (GY), Chemical Composition, and Static Water Contact Angle of the Functionalized PLA Surfaces

sample	reaction time (h)	GY[d] (μg/cm^2)	[N]/[C][e]	water contact angle (±3°)
pristine PLA				76
PLA-Br-1 from 1 h (or PLA-Br-12 from 12 h of aminolysis)[a]	1 (or 12)			73 (or 70)
PLA-*g*-P(MAA)1 from PLA-Br-1[b]	0.5	0.4 (±0.2)		57
PLA-*g*-P(MAA)1 from PLA-Br-12[b]	0.5	1.8 (±0.4)		51
PLA-*g*-P(MAA)2 from PLA-Br-12[b]	2	4.5 (±0.5)		49
PLA-*g*-P(MAA)1-gelatin from PLA-Br-1[c]	12	0.7 (±0.3)	0.11	52
PLA-*g*-P(MAA)1-gelatin from PLA-Br-12[c]	12	1.8 (±0.3)	0.14	45
PLA-*g*-P(MAA)2-gelatin from PLA-Br-12[c]	12	2.3 (±0.4)	0.18	46

[a] From the PLA-NH_2-1 (or PLA-NH_2-12) film which was obtained by immersing the pristine PLA film in 1,6-hexanediamine/2-propanol solution of 60 mg/mL for 1 (or 12) h at 40 °C. [b] Reaction conditions: [MAAS]:[CuBr]:[$CuBr_2$]:[PMDETA] = 100:1:0.2:1.2 in water at room temperature. [c] Obtained by immersing the corresponding PLA-*g*-P(MAA) surfaces in the PBS (pH 7.4) containing the gelatin at a concentration of 5.0 mg/mL at 40 °C. [d] Grafting yield (GY) is defined as GY = $(W_a - W_b)/A$, where W_a and W_b represent the weight of the dry films after and before grafting, respectively, and A is the film area (about 32 cm^2). [e] Determined from XPS.

[MAAS]:[CuBr]:[$CuBr_2$]:[PMDETA] was controlled at 100:1:0.2:1.2 (Table 1).

In this work, the grafting yield (GY) is defined as GY = $(W_a - W_b)/A$, where W_a and W_b are the weights of the dry film after and before graft copolymerization, respectively, and A is the film area. The respective GYs of P(MAA) from the PLA-Br-1, PLA-Br-6, and PLA-Br-12 surfaces at 0.5 and 2 h of ATRP were investigated in Figure S1 (see Supporting Information). The GYs of P(MAA) from the PLA-Br-1 surface were substantially lower than those from the PLA-Br-6 and PLA-Br-12 surfaces. As mentioned above, the initiator densities (ρ^*) of the PLA-Br-1, PLA-Br-6, and PLA-Br-12 surfaces are about 0.21, 1.26, and 1.52 initiators/nm^2, respectively. These above results indicate that the density of the initiation sites plays a very important role in achieving the high surface coverage of functional groups. The PLA-Br-6 and PLA-Br-12 surfaces with denser layers of immobilized ATRP initiators can increase the grafting density and produce a more complete surface coverage. On the other hand, there are no significant differences between the GYs of P(MAA) at a specific ATRP time from the PLA-Br-6 and PLA-Br-12 surfaces, probably due to the limited initiation sites required for surface-initiated ATRP. On the basis of the average cross-sectional area (about 2 nm^2) of methacrylate polymers grafted by "living" radical polymerizations,[31,33] the surface initiator efficiencies ($1/(2\rho^*)$) of the present PLA-Br-6 and PLA-Br-12 surfaces are estimated to be about 39% (from ρ^* = 1.26 initiators/nm^2) and 33%

(from ρ^* = 1.52 initiators/nm^2), respectively. It should be noted that the initiation efficiency is not reliably estimated because the actual initiation efficiency will depend very much on the reaction conditions, monomer type and reactivity, and molecular weight of the grafted polymer. Nevertheless, the above results confirmed that the more than 6 h of aminolysis in the present work is needed to produce the ATRP initiator-coupled surface with sufficient initiation sites.

Figure S2 (see Supporting Information) shows the C 1s core-level spectra of the PLA-*g*-P(MAA) surfaces. The C 1s core-level spectra (Figure S2a−c) of the PLA-*g*-P(MAA) surfaces from 0.5 h of ATRP can be curve-fitted into three peak components with BE's at about 284.6, 286.2, and 288.7 eV, attributable to the *C*−H, *C*−O, and O═*C*−O species, respectively.[29] The *C*−O peak component is associated with the underlying PLA substrate. The above XPS results indicated that the grafted P(MAA) layer from 0.5 h of ATRP on the PLA surface is less than the sampling depth (about 7.5 nm in an organic matrix[30]) of the XPS technique. The intensity of the *C*−O peak component of the PLA-*g*-P(MAA)1 surfaces from the PLA-Br-6 surface (Figure S2b) and the PLA-Br-12 surface (Figure S2c) is much lower than that of the PLA-*g*-P(MAA)1 surface from the PLA-Br-1 surface (Figure S2a), indicating that the PLA surfaces with denser layers of immobilized ATRP initiators can increase the grafting density. This result is consistent with that of Figure S1. When the ATRP time was extended to 2 h, no *C*−O peak component was observed on the PLA-*g*-P(MAA)2 surface from the PLA-Br-48 h surface (Figure S2d). The GY values for the PLA-*g*-P(MAA)1 and PLA-*g*-P(MAA)2 surfaces from the PLA-Br-48 surface are about 1.8 and 4.5 μg/cm^2, respectively (Table 1). The increased GY of the P(MAA) layer for the PLA-*g*-P(MAA)2 surface produce a more complete surface coverage, and the resultant thickness of the grafted P(MAA) layer has exceeded the sampling depth of the XPS technique, leading to the disappearance of the *C*−O peak component associated with the underlying PLA substrate. The average static water contact angles of the PLA-*g*-P(MAA) surfaces decreased to 49° from 70° (for the original PLA-Br-12 surface) (Table 1). The above results indicate that MAA has been successfully graft copolymerized onto the PLA-Br surface via surface-initiated ATRP. The molecular weight and molecular weight distribution of the surface-grafted polymer cannot be determined with sufficient accuracy without the cleavage of the grafted chains. It is very difficult, if not impossible, to precisely cleave the grafted P(MAA) chains from the PLA chains.

3.3. Immobilization of Gelatin and Cell Culture. Gelatin is mainly composed of denatured collagen, one naturally extracellular matrix protein. Gelatin has been widely used in tissue engineering because of its excellent cell adhesion, biodegradability, and superior biocompatibility in tissue replacement and wound healing.[10,26,27] The reactions of gelatin with the PLA-*g*-P(MAA) surfaces produced the corresponding gelatin-functionalized PLA surfaces (PLA-*g*-P(MAA)-gelatin surfaces), as shown in Figure 1 and Table 1. In the current work, the carboxylic acid groups of the PLA-*g*-P(MAA) surface were first converted into reactive esters (succinimidyl intermediates) in the presence of *N*-ethyl-*N*′-(3-(dimethylamino)propyl)carbodiimide (EDAC) and *N*-hydroxysuccinimide (NHS).[34] Then, the activated PLA-*g*-P(MAA) surface with the active intermediates was introduced into the gelatin solutions. The reactive esters underwent nucleophilic substitution reactions with the amine groups of gelatin to form a stable amide linkage without the presence of diimide, thus avoiding the intermolecular connection of proteins.

After the vigorous extraction of the reversibly and physically bound gelatin, their corresponding C 1s and N 1s core-level spectra of the (a, b) PLA-*g*-P(MAA)1-gelatin (from PLA-Br-1), (c, d) PLA-*g*-P(MAA)1-gelatin (from PLA-Br-6), and (e, f) PLA-*g*-P(MAA)2-gelatin (from PLA-Br-12) surfaces are shown in Figure S3 (see Supporting Information). The C 1s core-level spectra can be curve-fitted into five peak components with BE's at about 284.6, 285.7, 286.2, 287.4, and 288.4 eV, attributable to the *C*−H, *C*−N, *C*−O, O═*C*−N, and O═*C*−O species, respectively.[29] The *C*−N peak component is associated with the linkages in gelatin itself. The O═*C*−N peak component is associated with the peptide bonds in gelatin as well as linkages formed between the −COOH of P(MAA) and −NH$_2$ of gelatin molecules. The above results and the appearance of a strong N 1s signal at the BE of about 399.2 eV (Figure S3b,d,f), characteristic of the amine species,[28] are consistent with the fact that gelatin has been covalently immobilized on the PLA-*g*-P(MAA) surfaces.

The surface concentration of immobilized gelatin can be expressed as the [N]/[C] ratio (determined from the sensitivity factors-corrected N 1s and C 1s core-level spectral area ratio of the PLA-*g*-P(MAA)-Gelatin surfaces (Figure S3, Supporting Information). The denser −COOH groups of the grafted P(MAA) brushes played a dominant role in the immobilization of biomolecules. With the increase in the carboxyl concentration of the grafted P(MAA) layer, the concentration of covalently immobilized gelatin is expected to increase. For the PLA-*g*-P(MAA)1-gelatin (prepared from the PLA-Br-1 surface at 0.5 h of ATRP), PLA-*g*-P(MAA)1-gelatin (prepared from the PLA-Br-12 surface at 0.5 h of ATRP), and PLA-*g*-P(MAA)2-gelatin (prepared from the PLA-Br-12 surface at 2 h of ATRP) surfaces, the [N]/[C] ratios are about 0.11, 0.14, and 0.18, respectively (Figure S3 and Table 1). The corresponding immobilized amounts of gelatin are 0.7 (for the PLA-*g*-P(MAA)1-gelatin from the PLA-Br-1 surface), 1.8 (for the PLA-*g*-P(MAA)1-gelatin from the PLA-Br-12 surface), and 2.3 μg/cm^2 (for the PLA-*g*-P(MAA)2-gelatin from the PLA-Br-12 surface) (Table 1). In addition, the water contact angles of the PLA-*g*-P(MAA)-gelatin surfaces are also summarized in Table 1.

In this work, the 3T3 fibroblast cell line was used to evaluate the cell-adhesion properties of the pristine PLA, PLA-NH$_2$, PLA-gelatin, PLA-*g*-P(MAA), and PLA-*g*-P(MAA)-gelatin surfaces. The PLA-gelatin film surface was obtained from the PLA-NH$_2$ substrate surface (which can react with −COOH groups of gelatin) under the identical gelatin solutions for the preparation of the PLA-*g*-P(MAA)-gelatin surface. After the cell incubation, the surfaces were washed twice with the PBS solution to remove the dead and loosely attached cells. Figure S4 (see Supporting Information) shows the relative cell-adhesion density of 3T3 fibroblasts cultured for 12 h on the pristine PLA (as the control), PLA-NH$_2$-1, PLA-gelatin (from the PLA-NH$_2$-1 surface), PLA-*g*-P(MAA)1 (from the PLA-Br-1 surface), PLA-*g*-P(MAA)1-gelatin (from the PLA-Br-1 surface), PLA-*g*-P(MAA)1-gelatin (from the PLA-Br-12 surface), and PLA-*g*-P(MAA)2-gelatin (from the PLA-Br-12 surface) surfaces. In comparison with the gelatin-immobilized PLA surfaces, the pristine PLA, PLA-NH$_2$-1, and PLA-*g*-P(MAA)1 (from the PLA-Br-1 surface) surfaces exhibited poor cell attachments. It was reported that the PLA surfaces lack the good ability to interact with cells.[10−13] The anionically charged −COOH groups are also unfavorable to cell adhesion.[24] After the gelatin immobilization, the number of the

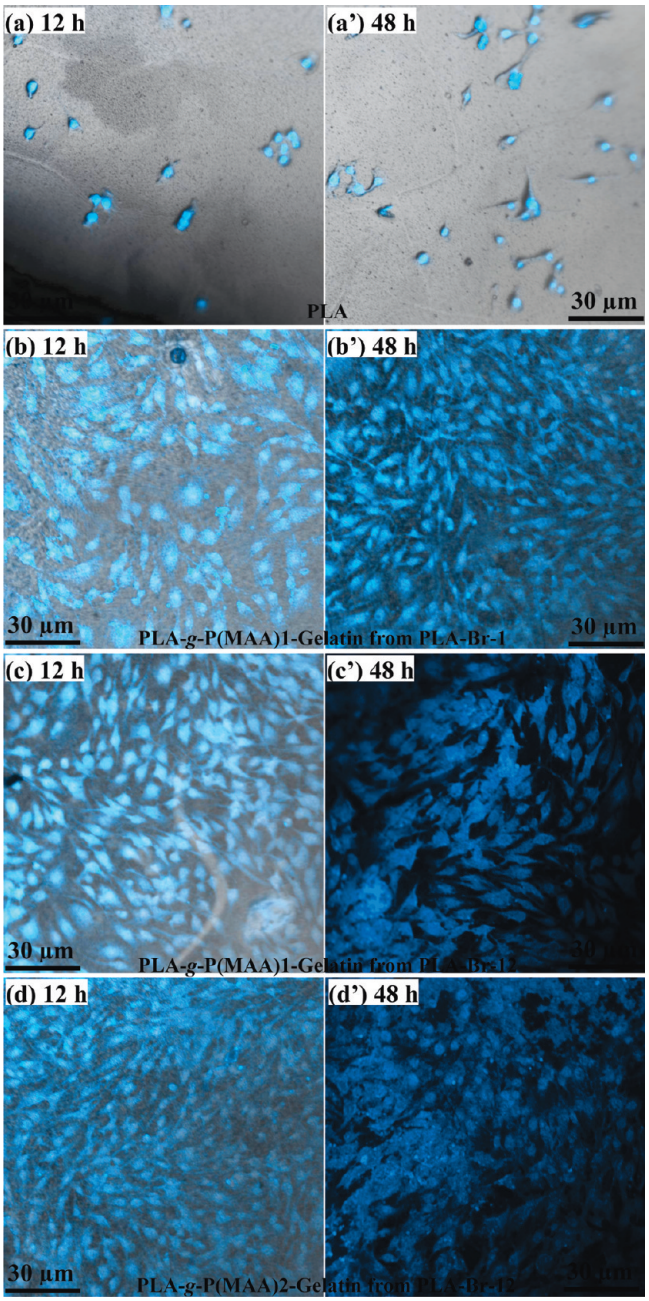

Figure 4. Optical images of 3T3 fibroblasts cultured for 12 and 48 h on the (a, a′) pristine PLA, (b, b′) PLA-*g*-P(MAA)1-gelatin (from the PLA-Br-1 surface), (c, c′) PLA-*g*-P(MAA)1-gelatin (from the PLA-Br-12 surface), and (d, d′) PLA-*g*-P(MAA)2-gelatin (from the PLA-Br-12 surface) surfaces.

attached cells on the functionalized PLA surfaces was enhanced substantially, arising from the bioactive components of gelatin. In comparison with the PLA-gelatin film surface (from the PLA-NH_2 substrate surface), the PLA-*g*-P(MAA)-gelatin surfaces, especially the PLA-*g*-P(MAA)1-gelatin (from the PLA-Br-12 surface) and PLA-*g*-P(MAA)2-gelatin (from the PLA-Br-12 surface) surfaces with the higher content of the immobilized gelatin, possess more pronounced enhancements in the density of attached cells. Gelatin is mainly composed of denatured collagen, one naturally extracellular matrix (ECM) protein. In general, the cell-adhesion process includes initial cell attachment to extracellular matrix (ECM), cell spreading, organization of an actin cytoskeleton, and formation of focal adhesions.[35,36] As each biomolecule can be covalently coupled to an individual −COOH group, the immobilized gelatin probably remains dispersed among the grafted P(MAA) chains, rather than forming a continuous surface layer. The higher content of the immobilized gelatin will produce a higher surface coverage. Thus, cell proliferation on the surface shows a positive correlation with the proportion of immobilized gelatin.

The morphologies of the attached cells on the functionalized PLA surfaces were also investigated by confocal laser scanning microscope (CLSM). Figure 4 shows the representative optical images of DAPI-stained 3T3 fibroblasts cultured for 12 and 48 h on the (a, a′) pristine PLA, (b, b′) PLA-*g*-P(MAA)1-gelatin (from the PLA-Br-1 surface), (c, c′) PLA-*g*-P(MAA)1-gelatin (from the PLA-Br-12 surface), and (d, d′) PLA-*g*-P(MAA)2-gelatin (from the PLA-Br-12 surface) surfaces. The PLA surface is unfavorable to cell attachment and growth. The higher the content of the immobilized gelatin, the higher the density of viable cells attached to the surface. These results are consistent with those of Figure S4 (see Supporting Information). It is obvious that coupling of gelatin onto the PLA surface has induced good cell adhesion and proliferation. The surfaces of the gelatin-functionalized PLA films are favorable to cell growth and survival. It is also possible to control the extent of cell immobilization on these modified PLA surfaces through adjusting of the gelatin content.

4. CONCLUSIONS

A simple two-step process was developed for the immobilization of ATRP initiators on the PLA film surfaces. The PLA film surfaces were successfully modified via surface-initiated ATRP of MAAS, followed by the attachment of gelatin on the P(MAA) brushes for enhancing the cell-adhesion properties. The amount of immobilized gelatin increases as that of the −COOH concentration of the grafted P(MAA) layer. The pristine PLA and PLA-*g*-P(MAA) surfaces are unfavorable to cell attachment and growth. The gelatin-functionalized PLA film surfaces exhibited excellent cell-adhesion characteristics. The higher the content of the immobilized gelatin, the higher the density of the viable cells attached to the surface. The dense pendant carboxyl groups of P(MAA) chains could provide much more binding sites of functional molecules to induce better cell-adhesion properties on the surface. With the inherent advantages of the good tissue biocompatibility of PLA substrates, the versatility of surface-initiated ATRP, and the good cell-adhesive nature of gelatin, the biomimetic surfaces of PLA scaffolds can be readily tailored to cater to different biomedical applications.

■ ASSOCIATED CONTENT

Supporting Information. Graft yield (GY) of the P(MAA) chains, XPS spectra of the PLA-*g*-P(MAA) and PLA-*g*-P(MAA)-gelatin, and cell-adhesion density of on the functionalized PLA films. This material is available free of charge via the Internet at http://pubs.acs.org.

■ AUTHOR INFORMATION

Corresponding Author
*E-mail: xufj@mail.buct.edu.cn.

■ ACKNOWLEDGMENT

This work was supported in part by National Natural Science Foundation of China (Grant No. 50903007), Fok Ying Tung Education Foundation (Project No. 121048), and Program for New Century Excellent Talents in University (NCET-10-0203).

■ REFERENCES

(1) Zhu, Y.; Gao, C.; Liu, X.; Shen, J. *Biomacromolecules* **2002**, *3*, 1312–1319.
(2) Oyane, A.; Uchida, M.; Choong, C.; Triffitt, J.; Jones, J.; Ito., A. *Biomaterials* **2005**, *26*, 2407–2413.
(3) Diaz-Quijada, G. A.; Wayner, M. D. D. *Langmuir* **2004**, *20*, 9607–9611.
(4) Yu, Q.; Zhang, Y.; Chen, H.; Zhou, F.; Wu, Z.; Huang, H.; Brash, J. H. *Langmuir* **2010**, *26*, 8582–8588.
(5) Xu, F. J.; Zhao, J. P.; Kang, E. T.; Neoh, K. G.; Li, J. *Langmuir* **2007**, *23*, 8585–8592.
(6) Janorkar, A. V.; Metters, A. T.; Hirt, D. E. *Macromolecules* **2004**, *37*, 9151–9159.
(7) Zhu, A.; Zhang, M.; Wu, J.; Shen, J. *Biomaterials* **2002**, *23*, 4657–4655.
(8) Zhu, H.; Ji, J.; Tan, Q.; Barbosa, M. A.; Shen, J. *Biomacromolecules* **2003**, *4*, 378–386.
(9) Yamashita, K.; Kikkawa, Y.; Kurokawa, K.; Doi, Y. *Biomacromolecules* **2005**, *6*, 850–867.
(10) Hou, X.; Zhang, B. L.; She, F.; Cui, Y. L.; Shi, K. Y.; Yao, K. D. *Chin. J. Polym. Sci.* **2003**, *3*, 277–283.
(11) Cai, K.; Yao, K.; Cui, Y.; Lin, S.; Yang, Z.; Li, X.; Xie, H.; Qing, T.; Luo, J. *J. Biomed. Mater. Res.* **2002**, *60*, 398–404.
(12) Kito, H.; Matsuda, T. *J. Biomed. Mater. Res.* **1996**, *30*, 321–330.
(13) Chu, F. L. C.; Lu, A.; Liszkowski, M.; Sipehia, R. *Biochim. Biophys. Acta* **1999**, *1472*, 479–485.
(14) Xu, F. J.; Li, Y. L.; Kang, E. T.; Neoh., K. G. *Biomacromolecules* **2005**, *6*, 1759–1768.
(15) Fu, L.; Chen, X.; He, J.; Xiong, C.; Ma, H. W. *Langmuir* **2008**, *24*, 6100–6106.
(16) Kusumo, A.; Bombalski, L.; Lin, Q.; Matyjaszewski, K.; Schneider., J. W.; Tilton, R. D. *Langmuir* **2007**, *23*, 4448–54.
(17) Ramstedt, M.; Cheng, N.; Azzaroni, O.; Mossialos, D.; Mathieu, H. J.; Huck, W. T. S. *Langmuir* **2007**, *23*, 3314–3321.
(18) Matyjaszewski, K.; Xia, J. H. *Chem. Rev.* **2001**, *101*, 2921–2990.
(19) Osborne, V. L.; Jones, D. M.; Huck, W. T. S. *Chem. Commun.* **2002**, *17*, 1838–1839.
(20) Tugulu, S.; Barbey, R.; Harms, M.; Fricke, M.; Volkmer, D.; Rossi, A.; Klok, H. A. *Macromolecules* **2007**, *40*, 168–177.
(21) Xu, F. J.; Wang, Z. H.; Yang, W. T. *Biomaterials* **2010**, *31*, 3139–3147.
(22) Xu, F. J.; Neoh, K. G.; Kang, E. T. *Prog. Polym. Sci.* **2009**, *34*, 719–761.
(23) Boyes, S. G.; Akgun, B.; Brittain, W. J.; Foster, M. D. *Macromolecules* **2003**, *36*, 9539–9548.
(24) Zhang, F.; Zhang, Z.; Zhu, X.; Kang, E. T.; Neoh, K. G. *Biomaterials* **2008**, *29*, 4751–4759.
(25) Zhu, Y.; Gao, C.; Liu, X.; He, T.; Shen, J. *Tissue Eng.* **2004**, *10*, 53–61.
(26) Vlierberghe, S. V.; Vanderleyden, E.; Boterberg, V.; Dubruel, P. *Polymers* **2011**, *3*, 114–30.
(27) Bratt-Leal, A. M.; Carpenedo, R. L.; Ungrin, M. D.; Zandstra, P. W.; McDevitt, T. C. *Biomaterials* **2011**, *32*, 48–56.
(28) Fischer, D.; Li, Y.; Ahlemeyer, B.; Krieglstein, J.; Kissel, T. *Biomaterials* **2003**, *24*, 1121–1131.
(29) Moulder, J. F.; Stickle, W. F.; Sobol, P. E.; Bomben, K. D. In *X-ray Photoelectron Spectroscopy*; Chastain, J., Ed.; Perkin-Elmer: Eden Prairie, MN, 1992; p 43.
(30) Tan, K. L.; Woon, L. L.; Wong, H. K.; Kang, E. T.; Neoh, K. G. *Macromolecules* **1993**, *26*, 2832–2836.
(31) Xu, F. J.; Zhao, J. P.; Kang, E. T.; Neoh, K. G. *Ind. Eng. Chem. Res.* **2007**, *46*, 4866–4873.
(32) Jeyaprakash, J. D.; Samuel, S.; Dhamodharan, R.; Rühe, J. *Macromol. Rapid Commun.* **2002**, *23*, 277–281.
(33) Shah, R. R.; Merreceyes, D.; Husemann, M.; Rees, I.; Abbott, N. L.; Hawker, C. J.; Hedrick, J. L. *Macromolecules* **2000**, *33*, 597–608.
(34) Jiang, K.; Schadler, L. S.; Siegel, R. W.; Zhang, X.; Zhang, H.; Terrones, M. *J. Mater. Chem.* **2004**, *14*, 37–39.
(35) Yang, X. B.; Bhatnagar, R. S.; Li, S.; Oreffo, R. O. C. *Tissue Eng.* **2004**, *10*, 1148–1159.
(36) Lebaron, R. G.; Athanasiou, K. A. *Tissue Eng.* **2000**, *6*, 85–103.